Effects of a Short-Chain Ceramide on Bilayer Domain Formation, Thickness, and Chain Mobililty: DMPC and Asymmetric Ceramide Mixtures

Dolores C. Carrer,* Shirley Schreier,† Martín Patrito,‡ and Bruno Maggio*
*Departamento de Química Biológica–CIQUIBIC and ‡Departamento de Físico-Química—INFIQC, Facultad de Ciencias Químicas, Universidad Nacional de Córdoba, Córdoba, Argentina; and †Instituto de Química, University de Sao Paulo, Sao Paulo, Brazil

ABSTRACT An important part of natural ceramides contain asymmetric hydrocarbon chains. We have used calorimetry, atomic force microscopy, and electron paramagnetic resonance to study the effect of ceramide chain asymmetry in mixtures of C8Cer with DMPC as a model system of hydrocarbon chain disparity. A phase diagram is provided along with information on the thickness of the membrane and the mobility of the chains at different temperatures both below and above the phase transition temperature of the mixtures. The results indicate a partial interdigitation of C8Cer chains in the gel phase, producing a correlation between the organization of both hemilayers. Our data suggest that the effects of ceramides on biomembranes may be bimodal and similar to those of cholesterol.

INTRODUCTION

Ceramide is a key signaling molecule, active in most eukaryotic cells. Different stress agents (radiation, heat shock, virus infection), along with cytokines like TNFα and IL-1β, produce a rise in ceramide membrane content, which in turn mediates responses like differentiation, proliferation, and apoptosis (1).

In the last few years, ceramide has been the object of biophysical studies that have provided some clues as to the molecular basis of its effects in membranes (2–7). Nonetheless, few studies have addressed the issue of the effects of ceramide chain heterogeneity on membrane organization.

A considerable proportion of natural ceramides contain long fatty acyl chains (C24–C26). This fact allows the hydrocarbon chain to protrude seven to nine carbon-carbon bond lengths from the sphingosine chain, as the latter does not penetrate more than 14–15 carbon-carbon bonds into the membrane (8,9). Such a high asymmetry makes possible the interdigitation of the hydrocarbon chains in the opposing membrane hemilayer. In turn, this possibility brings about consequences to the membrane organization, according to the number of asymmetric molecules present and the degree of asymmetry.

The effects of chain asymmetry in phospholipid bilayers have been meticulously studied by Huang and co-workers (10–12). These authors showed that the membrane organization can be predicted based on a parameter (the normalized chain asymmetry, $\Delta C/CL$) that quantifies the length difference of the hydrocarbon moiety. As defined in those studies, in this work we will use the term ''mixed-interdigitated'' to indicate a membrane in which the longer chain spans the whole width of the bilayer, whereas the shorter chains pack end to end. The term ''partially interdigitated'' will be used to describe a situation in which lipid molecules pack with the shorter chain end-to-end with the longer chain of the molecule in the opposing hemilayer (see Huang and Mason (10) and Fig. 8 in this article).

In previous work, it has been shown that asymmetric sphingolipids (cerebroside, sphingmyelin, gangliosides with 20–26 C fatty acyl residues) added in very small proportions to membranes formed mainly by symmetric phospholipids organize themselves so as to introduce the fatty acyl chain into the opposing hemilayer (13–16). When the proportion of asymmetric sphingolipid is increased above 40 mol %, the membrane adopts a partially interdigitated structure; when the sphingolipid represents >70% of the membrane, the latter adopts a mixed-interdigitated or partially interdigitated organization, depending on temperature (10,17–19).

Unlike the sphingolipids mentioned above, ceramide has a very small polar headgroup, which allows it to flip-flop rapidly from one hemilayer to the other in a membrane (20–23). This property should give ceramide the ability to form membrane spanning domains (with ceramide in both sides of the membrane) which, if sufficiently enriched in asymmetric molecules, could adopt a mixed-interdigitated conformation even at relatively low global ceramide concentration in the membrane.

To address this hypothesis, in this work we studied the effect of ceramide chain asymmetry on membrane organization in mixtures of ceramide with a symmetric phospholipid, dimiristoylphosphatidylcholine (DMPC). We used as a model system of hydrocarbon chain disparity *N*-octanoylsphingosine (C8Cer), frequently employed to study ceramide effects in cells (24,25). Although in this molecule the fatty acyl chain is shorter than the sphingosine (and not longer as in natural ceramides), it has the same degree of

Submitted September 14, 2005, and accepted for publication December 12, 2005.

Address reprint requests to Dolores C. Carrer, MEMPHYS–Centre for Biomembrane Physics, Physics Department, Campusvej 55 DK 5230, Odense M, Denmark. Fax: 45-6615-8760; E-mail: dcarrer@gmail.com.

0006-3495/06/04/2394/10 $2.00

doi: 10.1529/biophysj.105.074252

asymmetry as C24Cer ($\Delta C/CL = 0.38$–0.53), which should allow it to form a mixed-interdigitated membrane (19).

MATERIALS AND METHODS

C8Cer and DMPC were form Avanti Polar Lipids (Alabaster, AL). Spin-labeled fatty acids (5-, 12-, and 16-SASL) were from Sigma (St. Louis, MO). NaCl (from Merck, Darmstad, Germany) was submitted to high temperature (450°C for 3 h) to eliminate any organic contamination. Solvents from Merck were of the highest purity. Water was Mili-Q or twice distilled in a glass apparatus. In atomic force microscopy (AFM) experiments, muscovite mica was used. Cantilevers with Al coating and nominal force constant of 0.35 N/m were purchased from Molecular Imaging (Tempe, AZ).

Aqueous lipid dispersions were prepared by premixing the lipids in the desired proportions from solutions in 2:1 chloroform/methanol. The mixture was taken to dryness as a thin film in a conic tube under N_2 and submitted to high vacuum for at least 4 h. Multilamellar vesicles (MLV) were obtained by hydrating the dry lipid with 145 mM NaCl and subsequent freeze-thaw-vortexing from −180°C to 90°C at least four times. For AFM experiments, the MLV were extruded through polycarbonate membranes (0.1-μm pore diameter) at ~65°C to obtain large unilamellar vesicles (LUVs) 80 ± 30 nm in diameter. Vesicle size was assessed by dynamic light scattering making use of a Nicomp submicron particle sizer (Santa Barbara, CA). The ceramide-enriched samples (30 mol %) had to be incubated at 30°C overnight before extrusion to obtain unilamellar vesicles. These samples had a tendency to remain as multilamellar vesicles despite the extrusion.

For calorimetry, the MLV dispersion was degassed under low pressure and introduced in the sample cell of a high sensitivity Microcal differential scanning calorimeter (Northampton, MA). The reference cell was filled with 145 mM NaCl. The proportion of Cer in the mixtures varied between 0 and 30 mol %; whereas the concentration of DMPC was kept constant at 3.0 mM, the total amount of lipid varied between 3.0 and 4.63 mM. Samples were run at 30°C/h duplicate.

To prepare the AFM samples, a small volume (20–220 μl) of LUV (extruded, 80 ± 20 nm in diameter) suspension was incubated at variable times (30 s to 30 min) over freshly cleaved mica in a teflon cell at the desired temperature. After carefully rinsing with pure water, the samples were observed with a PicoScan AFM-STM microscope under water (Molecular Imaging). The temperature was controlled using an air conditioner.

For electron paramagnetic resonance (EPR) experiments, 5 mM MLV containing 1 mol % spin-labeled stearic acid was prepared as described before, using 145 mM NaCl with 20 mM sodium acetate buffer (pH 4.5) as the hydrating solution (9). EPR spectra were recorded on a Bruker spectrometer (Madison, WI) equipped with a nitrogen-flow temperature controller. Duplicate or triplicate spectra were taken with different samples each time. For each spectrum, four to eight spectra were recorded and added.

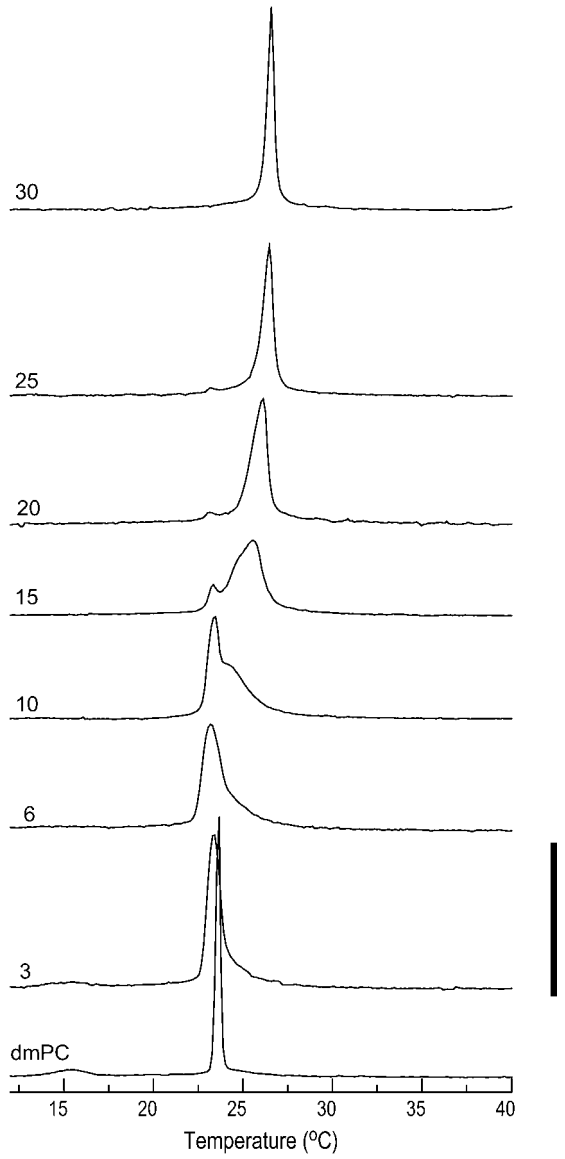

FIGURE 1 Calorimetric data for DMPC-C8Cer mixtures. Normalized heat capacity versus temperature curves are shown for DMPC-C8Cer mixtures (second heating scan). The figures in the curves indicate, in mol %, the amount of C8Cer in the mixtures. The ordinate values of the DMPC curve are shown multiplied by 0.5. The bar indicates 5 kcal/(K·mol).

RESULTS

Calorimetric phase diagram

Fig. 1 shows the calorimetry curves of DMPC-C8Cer mixtures containing up to 30 mol % of the latter. Very small amounts of C8Cer produce considerable changes in $\Delta C_{p\text{-}max}$, indicating a steep fall of the transition cooperativity. For example, $\Delta C_{p\text{-}max}$ decreases from 17.7 kcal/K·mol for pure DMPC to 5.2 kcal/K·mol for the sample containing 3 mol % C8Cer (Fig. 1).

The curves in Fig. 1 show the presence of two peaks. The first remains fixed at a temperature very near that of pure DMPC phase transition and loses importance until it vanishes in samples with 30 mol % C8Cer. The second peak appears as a high-temperature asymmetry of the first one, then as a shoulder, and finally as the main, and subsequently only, peak in the 30-mol % C8Cer sample. The relative contribution of each peak can be appreciated also in Fig. 2, where T_m (the temperature of $\Delta C_{p\text{-}max}$) is shown for each sample.

As seen in the partial phase diagram (Fig. 2), incorporation of small amounts of C8Cer lowers the phase transition temperature of DMPC. This may represent autectic phase behavior, a characteristic feature of systems exhibiting partially interdigitated hydrocarbon chains. After that initial depression, T_S (the temperature at which the phase transition begins) remains practically constant between C8Cer mole

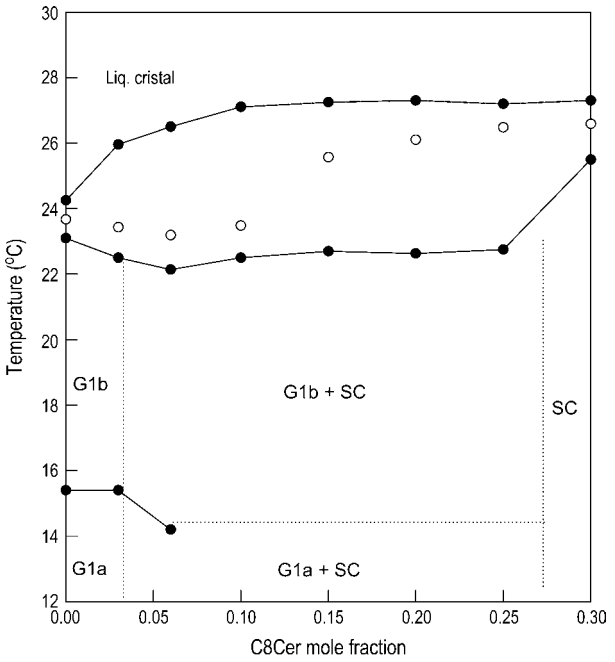

FIGURE 2 Partial calorimetric phase diagram of DMPC-C8Cer mixtures. Calorimetrically determined T_p, T_S, T_L (*solid symbols*), and T_m (*open symbols*) are shown for mixtures of DMPC and C8Cer up to 30 mol % of the latter. *G1a*, gel phase 1a; *G1b*, gel phase 1b; and *SC*, stoichiometric compound.

fractions of 0.03 and 0.25. At a mole fraction of 0.30, T_S rises by >2°C. The presence of only one peak at 30 mol % C8Cer indicates that at this composition the membrane is formed by a single gel phase; that is, the 30-mol % C8Cer mixture behaves as a stoichiometric compound. The fact that the temperature at the beginning of the phase transition is constant and practically the same as that of pure DMPC between 3 and 25 mol % C8Cer, as revealed by the presence of a horizontal line for T_S in the phase diagram, indicates that in this range of compositions, part of the membrane is laterally segregated in gel-phase domains formed by DMPC saturated by ~3 mol % C8Cer. From this proportion, C8Cer is incorporated in a second gel phase of composition equal to the stoichiometric compound (~70:30 DMPC/C8Cer). As a result, the relative quantities of each phase change as the proportion of C8Cer changes in the mixture; for example, between 10 and 15 mol % of C8Cer, ~50% of lipid molecules form the DMPC-enriched phase, whereas the remaining molecules form the phase with 30 mol % C8Cer. The presence of a horizontal line in T_L (the temperature at which the phase transition ends) from 10 mol % C8Cer up to 30 mol % C8Cer suggests also the presence of coexisting liquid phases in this composition range.

AFM imaging of the gel phase

To elucidate whether these membranes form domains of different thickness in the gel phase, we examined pure DMPC membranes and mixtures with 10 and 30 mol % C8Cer at temperatures below the phase transition (15–20°C) by AFM. Fig. 3 shows representative images of LUVs adsorbed on mica. Gel-phase pure DMPC membranes have a thickness of ~5.0 nm, in agreement with previous reports (26). In the 10-mol % C8Cer sample, according to the calorimetric data, the total lipids would be distributed as 67% DMPC and 33% 70:30 DMPC/C8Cer complex. However, the membranes with 10 mol % C8Cer did not demonstrate coexistence of

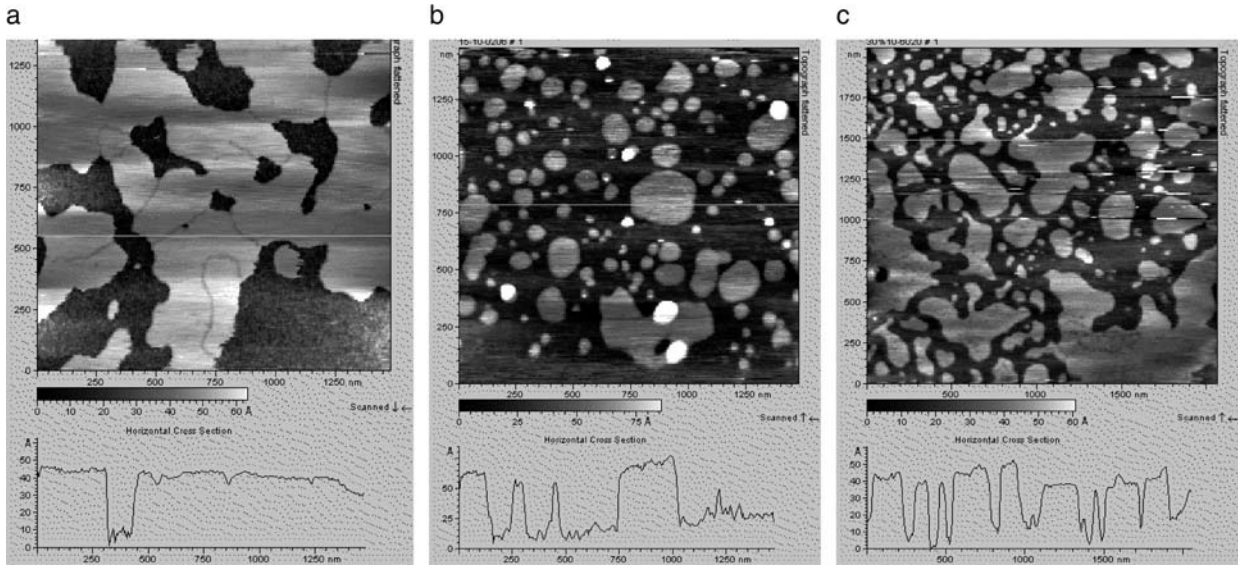

FIGURE 3 Atomic force microscopy images of DMPC-C8Cer bilayers on mica. Representative AFM images of pure DMPC (*a*), and 10- (*b*) and 30-mol % C8Cer (*c*) bilayers adsorbed to mica are shown. The samples were prepared and observed at temperatures corresponding to the gel phase. Note, in *a*, the defects formed by the incomplete fusion of adjacent patches of bilayer. In *b*, the white spots are the result of the adsorption of a second layer of LUVs to the substrate.

domains with different thickness, distinguishable with certainty form noise and baseline drift. These membranes showed an average thickness of 4.5–5.0 nm (Fig. 3).

The observation of membranes with 30 mol % C8Cer was more complicated. Once supported on the mica as single bilayers, these samples were difficult to image, probably because of the adhesion of material to the cantilever tip. From a series of preliminary images, we reported the presence of domains with thicknesses of ~2.4 and ~4 nm (27). Nonetheless, subsequently we only observed a homogeneous thickness of 4.0–4.5 nm. A possible explanation for this variability is the fact that, when the first images were obtained, the samples were maintained under observation for a long time (~5 h) until a reasonable level of noise and contrast was achieved. It is likely that during that time the mica-adsorbed membrane suffered a process of lipid loss to the aqueous phase. The formation of small defects in the adsorbed bilayer can produce lateral pressure fluctuations that could favor the formation of an interdigitated, thinner phase. In the mixed-interdigitated phase, the area per molecule increases, allowing for the healing of defects produced by the loss of lipid molecules to bulk water. An effect like this has been previously reported for dipalmitoyl phosphatidylcholine membranes adsorbed on mica (28). The AFM experiments described here, done under controlled exposure times, revealed thicknesses that varied between 4.0 and 5.0 nm for the gel phase of the samples studied, suggestive of noninterdigitated membranes.

Assesment of chain mobility by EPR

EPR is a very convenient tool to assess lipid interdigitation since it provides information on chain mobility at different depths of the membrane (17,29). EPR spectra were obtained for 5-, 12-, and 16-SASL incorporated in DMPC containing 0, 15, and 30 mol % C8Cer at different temperatures.

To be able to compare rigid spectra where inner hyperfine splitting is too small to be resolved, the outer splitting A// has been used as an empirical parameter. For spectra where the high mobility makes it impossible to resolve the outer and inner splitting, the quotient h_{+1}/h_0 has been used as indicative of mobility.

Fig. 4 shows data on the mobility of 5-SASL incorporated into different samples as a function of temperature. The data for 5-SASL incorporated into DMPC membranes shows a slow decrease in A// as the temperature rises in the gel phase, a steep decrease at the phase transition (indicated in the temperature axis), and again a slow decrease in the fluid phase (Fig. 4 *a*). This is a typical behavior for a pure saturated phosphatidylcholine membrane (30). The temperature of the chain-melting transition as revealed by EPR coincides with great accuracy with that measured by calorimetry. For 5-SASL incorporated into membranes containing 15 mol % C8Cer, the outer splitting decreases rapidly from 10°C to the values at 31°C in the fluid phase (Fig. 4 *b*). The phase transition is not as sharply indicated as in the case of pure DMPC membranes, and the outer splitting at temperatures below the phase transition is much lower than the DMPC or 30 mol % values (Fig. 4 *d*). For 5-SASL incorporated into 30-mol % C8Cer membranes, A// decreases slowly in the gel phase from 10 to 19°C, and then steeply while approaching the phase transition temperature (Fig. 4 *c*). Notably, the mobility of the probe in this mixture suggests that the chain-melting transition occurs at a temperature lower than the calorimetric transition. In the fluid phase at 31°C, 5-SASL shows a larger outer splitting in the 30% C8Cer sample than in the pure DMPC sample (Fig. 4 *d*). This is seen also at 10°C in the gel phase.

Fig. 5 shows data on the mobility of 16-SASL incorporated into different samples as a function of temperature. A// decreases as the temperature rises in the gel phase of DMPC and its mixtures with C8Cer at 15 and 30 mol %. For 16-SASL in pure DMPC, at the temperature corresponding to the phase transition, the spectra become too mobile for A// to be resolved, and then h_{+1}/h_0 is shown as indicative of mobility. This parameter increases rapidly with increasing temperature just above the phase transition and then more slowly afterwards. This same pattern is found for 15- and 30-mol % C8Cer samples, although ceramide-containing samples reach high mobility at temperatures lower than those of their phase transitions; that is to say, the mobility increases conspicuously before reaching the calorimetric phase transition and is already very similar to that of the fluid phase at temperatures still corresponding to the gel-fluid coexistence region according to calorimetry measurements. This coincides with the results obtained from 5-SASL in these same membranes (see Discussion). As can be seen in Fig. 5 *d*, the gel phase of the 30 mol % C8Cer sample shows smaller outer splitting than the pure DMPC sample. When 16-SASL is incorporated into the 15-mol % c8Cer sample, it shows an order parameter lying between those of DMPC and 30-mol % C8Cer (Fig. 5 *d*, *inset*). In the fluid phase at 31°C, the 30-mol % C8Cer sample is less mobile than the pure DMPC sample (Fig. 5 *d*).

Fig. 6 shows spectra obtained from 5-, 12-, and 16-SASL incorporated into 30-mol % C8Cer samples in the gel phase. As can be seen also from the A// values in Figs. 4 and 5, the outer hyperfine splitting values of 16-SASL spectra are much lower than for 5-SASL, which rules out the possibility of a mixed-interdigitated conformation in the C8Cer-enriched complex. A mixed-interdigitated conformation should restrict the motion of 16-SASL to values close to those of 5-SASL.

Fig. 7 shows data on the mobility of 12-SASL incorporated into mixed membranes. The outer splitting is measurable only up to the phase transition temperature of each sample. At higher temperatures, the parameter h_{+1}/h_0 is shown. The outer splitting of 12-SASL in gel-phase DMPC membranes falls slowly at low temperatures and then more rapidly near the phase transition temperature. In 30-mol % C8Cer samples,

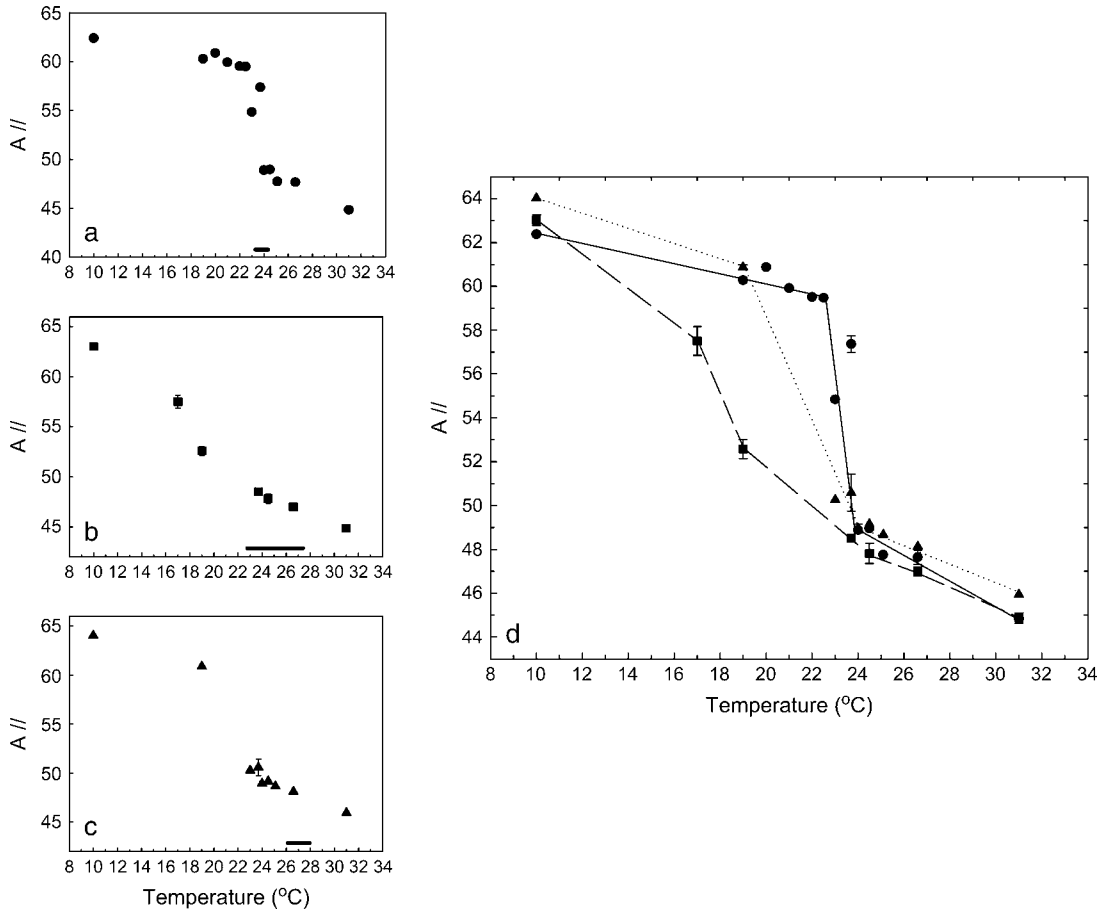

FIGURE 4 EPR data on 5-SASL incorporated in mixed DMPC-C8Cer membranes. Outer hyperfine splitting values are shown as a function of temperature for 5-SASL incorporated into DMPC membranes containing 0 mol % (*a*), 15 mol % (*b*), and 30 mol % C8Cer (*c*). On the temperature axis, the temperature range of the phase transition of each sample as determined by calorimetry is shown. (*d*) The same data for DMPC (*circles, solid line*) and 15-mol % (*squares, dashed line*) and 30-mol % C8Cer (*triangles, dotted line*) are shown together for comparison. The lines are drawn as a guide to the eye and do not represent an exact fit to the data. The error bars that cannot be seen are of the size of the data points or less.

on the other hand, the outer splitting remains practically constant and equal to the values at 10°C up to the phase transition temperature (Fig. 7 *c*). In the fluid phase of DMPC, the parameter h_{+1}/h_0 rises quickly from the phase transition and reaches a plateau around 30°C (Fig. 7 *a*). In 30-mol % C8Cer samples, however, this parameter remains at much lower values in the fluid phase (Fig. 7 *d*). When incorporated into 15-mol % samples, 12-SASL behaves in a way qualitatively more similar to DMPC than to the 30-mol % C8Cer complex. Two components are seen in spectra corresponding to the phase transition temperature of DMPC and 15- and 30-mol % C8Cer samples, probably due to gel-fluid phase coexistence.

DISCUSSION

At temperatures just below the phase transition, the 30-mol % sample as sensed by 5-SASL is much more mobile than the phosphatidylcholine (PC) gel phase, resembling the mobility of the fluid phase (Fig. 4). The chain-melting transition as reflected by EPR data seems to occur before the calorimetric transition. In the case of this probe, it may reflect a preferential partition of the probe to parts of the bilayer that begin to disorder as the phase transition temperature is approached, since the nitroxide is situated in an ordered region of the bilayer. However, a similar result is seen for 16-SASL incorporated into ceramide-containing samples. Others have reported a similar behavior for phosphatidylethanolamine spin probes incorporated in phosphatidylethanolamine-losartan membranes (31) and for pure phosphatidylethanolamine membranes studied by NMR spectroscopy (32). This may prove to be a general behavior for lipids with small and/or poorly hydrated polar groups.

As seen in Fig. 4 *d*, 5-SASL shows a smaller mobility in the 30-mol % C8Cer complex than in DMPC at temperatures below the pretransition and in the fluid phase. This probe shows instead a much greater mobility in the gel phase of the 15-mol % C8Cer sample than either in pure DMPC or in the 30-mol % C8Cer complex. This pattern in the 15-mol % mixture is quite perplexing, as this sample, as revealed by

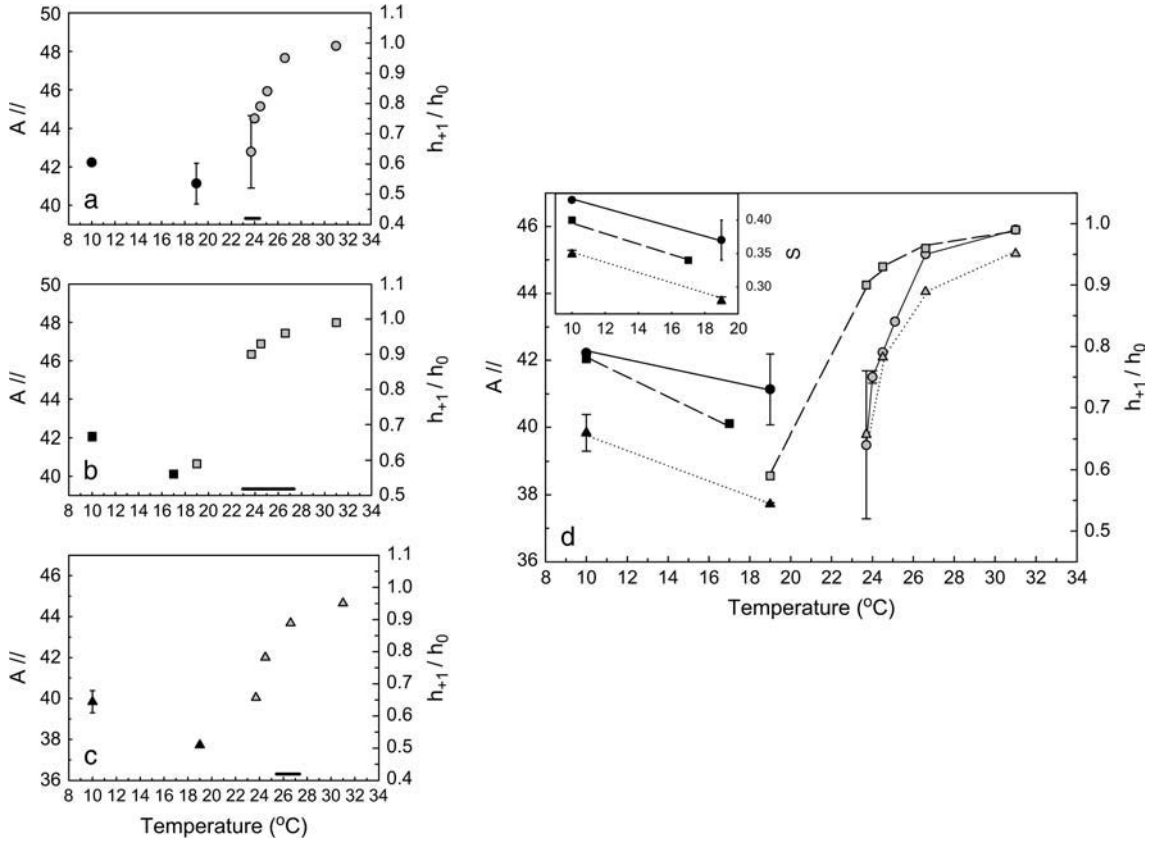

FIGURE 5 EPR data on 16-SASL incorporated in mixed DMPC-C8Cer membranes. Outer hyperfine splitting values (*solid symbols*) and h_{+1}/h_0 (*shaded symbols*) are shown as a function of temperature for 16-SASL incorporated into DMPC membranes containing 0 mol % (*a*), 15 mol % (*b*), and 30 mol % C8Cer (*c*). On the temperature axis, the temperature range of the phase transition of each sample as determined by calorimetry is shown. (*d*) The same data for DMPC (*circles, solid line*), and 15-mol % (*squares, dashed line*) and 30-mol % C8Cer (*triangles, dotted line*) are shown together for comparison. The lines are drawn as a guide to the eye and do not represent an exact fit to the data. The inset in *d* shows the order parameter as a function of temperature, calculated from the outer and inner splittings of the spectra (see Hoffman et al. (9) for details). The error bars that cannot be seen are of the size of the data points or less.

calorimetry, contains two coexisting phases: DMPC-enriched and 30-mol % C8Cer complex. The high mobility of 5-SASL may be related to the presence in the plane of the bilayer of coexisting domains with different packing properties (see below). Thus, the probe may be sensing defects brought about by the different packing constraints of the domains in the gel phase that allow for higher chain mobility.

The 30-mol % C8Cer stoichiometric compound probably has a different organization than the DMPC-enriched phase. The large polar group of PC has a larger area than the two hydrocarbon chains and thus produces a packing ''frustration'' that in pure gel-phase PC membranes is relieved by a tilting of the hydrocarbon chains and the formation of ripples at temperatures near the phase transition (33). The packing frustration can be minimized also by the addition of molecules bearing long hydrocarbon chains and small polar groups, removing chain tilt (34). Ceramide, having a very small polar group and a much smaller cross-sectional area than PC (~38 vs. ~50 Å^2), is able to abolish crowding of the headgroups and chain tilt while allowing for a tighter chain packing. As we will see below, this analysis explains the ordering effect of C8Cer at all depths in the fluid phase and near the interface region in the gel phase of mixed membranes. The coexistence of Cer-enriched domains (tightly packed, not tilted) with DMPC-enriched domains (with packing frustration relieved by chain tilt and/or ripple phase formation) could produce packing defects at boundaries between domains and probably also within the domains themselves. We do not have direct evidence to indicate the presence of tilted chains in the DMPC-enriched phase, although the persistence of the pretransition up to ~6 mol % C8Cer suggests that DMPC-enriched domains may still have tilted chains. This may be an explanation for the increased disorder sensed by 5-SASL in membranes containing 15 mol % C8Cer and showing coexistence of PC- and C8Cer-enriched gel-phase domains.

The spectra from 16-SASL show that the 30-mol % complex is more mobile than DMPC in the gel phase and less mobile in the fluid phase (Fig. 5). The 15-mol % sample shows an order parameter that lies between those of DMPC and the 30-mol % complex in the gel phase. This indicates that the probe is exchanging fast between the two coexisting

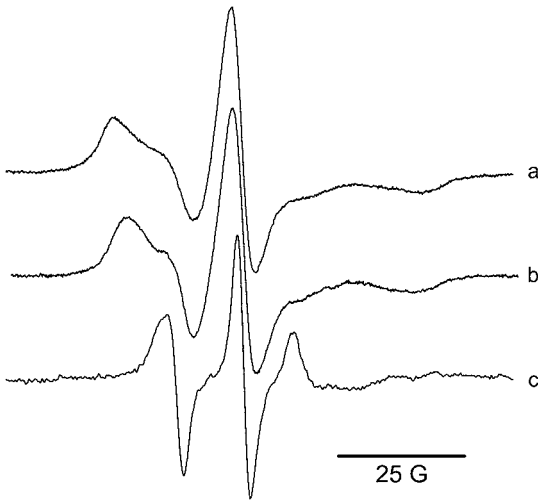

FIGURE 6 EPR spectra of fatty acid spin labels incorporated into DMPC-C8Cer bilayers in the gel phase. EPR spectra of 5- (*a*), 12- (*b*), and 16-SASL (*c*) in 30-mol % C8Cer membranes are shown. All spectra are taken at 19°C.

phases, and so the order parameter is a weighted sum of the order parameters of the two phases.

The mobility of 16-SASL in the 30-mol % C8Cer sample is much larger than that of 5-SASL in this same sample (Fig. 6). This rules out the possibility of a mixed-interdigitated conformation. If the sphingosine chain were spanning the entire width of the bilayer, 16-SASL should have a motional restriction close to that of 5-SASL. Our results indicate instead that the nitroxide group of 16-SASL is lying deep in the bilayer and not near the interface region. This inability of C8Cer to induce a mixed-interdigitated conformation despite its high degree of chain asymmetry is probably due to the fact that it represents only 30% of the molecules in the Cer-enriched phase.

The data on 12-SASL incorporated into the mixtures show that the 30-mol % C8Cer complex is less mobile than DMPC in the gel phase, especially at temperatures over the pretransition of DMPC (Fig. 7 *d*). The outer splitting of 12-SASL is only slightly smaller than that of 5-SASL in this sample (Fig. 6), and so the mobility gradient in the complex is partially lost. This may indicate partially interdigitated chains (see Fig. 8) sensed by this probe (17). In the fluid phase, 30-mol % C8Cer is also more ordered than DMPC (Fig. 7 *d*), which coincides with data obtained from 5- and 16-SASL. The higher conformational order at all depths sensed in the fluid phase of Cer-enriched samples is consistent with previous data from fluorescence and ^{2}H-NMR spectroscopy (35,36).

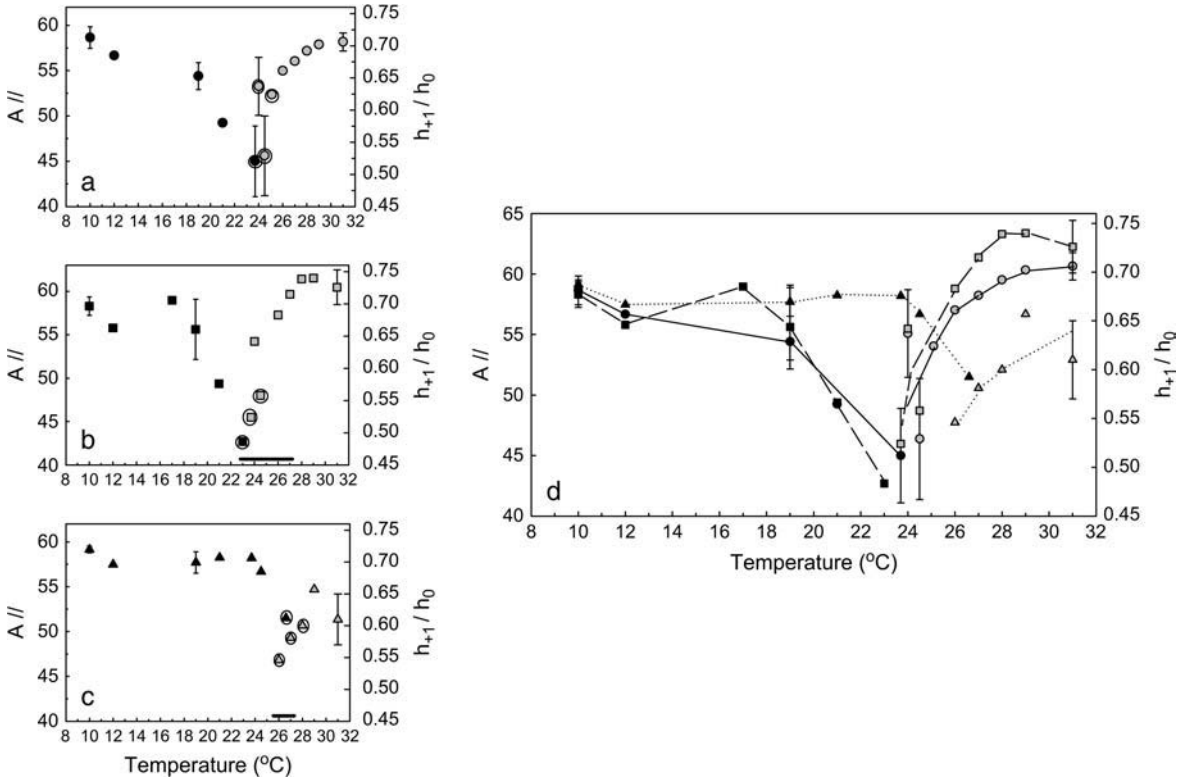

FIGURE 7 EPR data on 12-SASL incorporated into mixed DMPC-C8Cer membranes. Outer hyperfine splitting values (*solid symbols*) and h_{+1}/h_0 (*shaded symbols*) are shown as a function of temperature for 12-SASL incorporated into DMPC membranes containing 0-mol % (*a*), 15-mol % (*b*), and 30-mol % C8Cer (*c*). On the temperature axis, the temperature range of the phase transition of each sample as determined by calorimetry is shown. The circles around the data points indicate the presence of two components in the spectrum. Only the data of the major component is shown in the graph. (*d*) The same data for DMPC (*circles, solid line*), and 15-mol % (*squares, dashed line*) and 30-mol % C8Cer (*triangles, dotted line*) are shown together for comparison. The lines are drawn as a guide to the eye and do not represent an exact fit to the data. The error bars that cannot be seen are of the size of the data points or less.

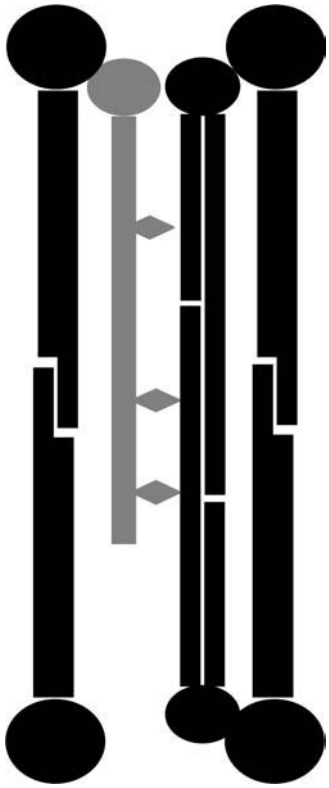

FIGURE 8 Schematic model of the chain organization of the 7:3 DMPC/C8Cer complex in the gel phase. Lipid molecules are shown in black, with C8Cer (small polar headgroup) having partially interdigitated chains. The three positions of the nitroxide group in the spin labels used are shown in gray.

As a general conclusion from the data obtained at different positions of chain labeling in the fluid phase, it can be interpreted that the 30-mol % C8Cer complex is more ordered than DMPC not only near the interface region but also deep in the hydrocarbon core in the regions sensed by 12- and 16-SASL. This correlates with previous data (35,36) while giving a more detailed picture of Cer effects in the fluid phase. As discussed above, this ordering effect of C8Cer can be explained by its small polar group, which allows for a tighter chain packing. Cer might also be able to adopt a superlattice organization, thus further minimizing membrane free volume (for a review on superlattice organization, see Somerharju et al. (37)).

The data on the gel phase of the mixtures is more complex. Let us consider the 30-mol % C8Cer complex. C8Cer produces a decreased mobility in this sample compared to pure DMPC near the interface and in the region sensed by 12-SASL, but increases chain disorder and mobility as sensed by 16-SASL. This apparently contradictory effect of C8Cer can be explained by the induction of a partially interdigitated structure in the gel phase of the C8Cer-enriched membrane. Fig. 8 shows our model of the C8Cer-enriched membrane organization. In the 30-mol % C8Cer complex, the Cer molecules would adopt a partially interdigitated structure. In this case, 5-SASL senses an increased molecular packing due to the small polar group of Cer, whereas 12-SASL would be sensing a diminished mobility of the sphingosine chain due to the interdigitation, and 16-SASL should sense an increased disorder due to the vicinity of the nitroxide group to a region near the bulky terminal methyl groups of both DMPC and C8Cer. It is interesting to note that the formation of a partially interdigitated structure in the presence of C8Cer indicates a correlation between the organization of both hemilayers that may have important consequences if it were to occur in a cell membrane.

Data obtained in this and previous works (2,3) on the calorimetric transition temperatures and enthalpies of Cer-enriched samples led us to the following observation: in membranes enriched in asymmetric ceramides (such as naturally occurring ceramides), the phase-transition entropies are relatively low compared to those of symmetric PCs, even with ceramides bearing long *N*-acyl chains. Table 1 shows some of these entropy values normalized by the expected entropy change (10). There exist three possibilities that would explain the decreased transition entropy: either the gel phase of the ceramide-enriched membranes are disordered by ceramides, or the fluid phases are ordered by ceramides, or both effects occur. The data obtained in this study suggest that asymmetric ceramides probably produce both a disordering of the gel phase and an increased ordering of the fluid phase when mixed with symmetric PCs. This conclusion is in agreement with data obtained by others (35,36,38–41) and by us (27). The experimental evidence then suggests that the gel phase is disordered due to ceramide-chain mismatch and/or heterogeneity (in the case of naturally ocurring ceramides), which does not allow the chains to adopt a conformation maximizing chain-chain interaction for all the different *N*-acyl chain lengths present, and due to the induction of gel-gel phase coexistence and the presence of bulky terminal methyl groups in a wider volume than normal (in the case of both naturally occurring ceramides and C8Cer). The fluid phase has a higher degree of packing density, microviscosity and order due to the small size and low hydration of the polar head of ceramides, that allows for tighter chain-chain interactions. The effect of

TABLE 1 Thermodynamic parameters for ceramide-containing bilayers

X_{C8Cer}*	T_m (°C)	ΔH (kcal/mol)	$\Delta S/\Delta S_{exp}$	$X^{\dagger}_{BBCer}$	T_m (°C)	ΔH (kcal/mol)	$\Delta S/\Delta S_{exp}$
0 (DMPC)	23.67	7.4	0.47	0 (DPPC)	40.93	8.4	0.44
0.06	23.19	6.9	0.44	0.04	41.77	8.1	0.42
0.15	25.57	6.3	0.41	0.16	42.43	7.4	0.38
0.25	26.48	5.8	0.38	0.20	43.07	6.5	0.33
0.30	26.59	4.9	0.32	0.30	52.07	6.1	0.30

The transition entropy $\Delta S = (\Delta H/T_m)$ is normalized by the expected transition entropy $\Delta S_{exp} = (1.9 \text{ eu/mol } (n1 + n2))$ (10). BBCer, bovine brain ceramide; DPPC, dipalmitoyl phosphatidylcholine. *Molar fraction of C8Cer. †Molar fraction of BBCer (data on mixtures of DPPC and BBCer obtained in previous work (2)).

ceramide-chain mismatch would be less important in the fluid phase, where all chains already have higher configurational disorder, than in the gel phase, where packing defects brought about by chain asymmetry would force the chains to adopt a more disordered conformation.

These considerations disclose an interesting phenomenon: naturally occurring ceramides appear to have a bimodal effect and may act in a way similar to cholesterol, making gel phases more fluid-like and fluid phases more gel-like. Also, natural ceramides are able to induce the persistence of gel phase domains at high, physiologically relevant temperatures (2,35). These gel phases would be, however, more fluid-like than an ordinary phospholipid gel-phase domain. These particular characteristics of ceramide-enriched domains could have important implications in ceramide-mediated signal transduction in cells.

D.C.C. was Postdoctoral Fellow of the Fundación Antorchas and Doctoral Fellow of Consejo Nacional de Investigaciones Científicas y Técnicas while producing this work. B.M. is Investigador Superior of Consejo Nacional de Investigaciones Científicas y Técnicas. S.S. is Full Professor at University of Sao Paulo. M.P. is Investigador Adjunto of Consejo Nacional de Investigaciones Científicas y Técnicas.

This work was supported by grants conferred by the Fundación Antorchas, Fondo Nacional de Ciencia y Técnica, Secretaría de Ciencia y Técnica-Universidad Nacional de Córdoba, Fundação de Amparo à Pesquisa do Estado de São Paulo. D.C.C. thanks Universidade da São Paulo for financial support of her stay in São Paulo. S.S. has a research fellowship from Conselho Nacional de Desenvolvimento Científico e Tecnológico.

REFERENCES

1. Hannun, Y. A., and C. Luberto. 2000. Ceramide in the eukaryotic cell response. *Trends Cell Biol.* 10:73–80.
2. Carrer, D. C., and B. Maggio. 1999. Phase behavior and molecular interactions in mixtures of ceramide with dipalmitoylphosphatidylcholine. *J. Lipid Res.* 40:1978–1989.
3. Carrer, D. C., and B. Maggio. 2001. Transduction to self-assembly of molecular geometry and local interactions in mixtures of ceramides and ganglioside GM1. *Biochim. Biophys. Acta.* 1514:87–99.
4. Maggio, B., D. C. Carrer, M. L. Fanani, R. G. Oliveira, and C. M. Rosetti. 2004. Interfacial behavior of glycosphingolipids and related sphingolipids. *Curr. Opin. Colloid Interface Sci.* 8:448–458.
5. Holopainen, J. M., M. Angelova, and P. K. J. Kinnunen. 2000. Vectorial budding of vesicles by asymmetrical enzymatic formation of ceramide in giant liposomes. *Biophys. J.* 78:830–838.
6. Veiga, M. P., J. L. Arrondo, F. M. Goñi, and A. Alonso. 1999. Ceramides in phospholipid membranes: effects on bilayer stability and transition to nonlamellar phases. *Biophys. J.* 76:342–350.
7. Contreras, F. X., A. V. Villar, A. Alonso, R. N. Kolesnick, and F. M. Goñi. 2003. Sphingomyelinase activity causes transbilayer lipid translocation in model and cell membranes. *J. Biol. Chem.* 278:37169–37174.
8. Pascher, I., M. Lundmark, P.-G. Nyholm, and S. Sundells. 1992. Crystal structures of membrane lipids. *Biochim. Biophys. Acta.* 1113: 339–373.
9. Hoffmann, P., K. Sandhoff, and D. Marsh. 2000. Comparative dynamics and location of chain spin-labeled sphingomyelin and phosphatidylcholine in dimiristoyl phosphatidylcholine membranes studied by EPR spectroscopy. *Biochim. Biophys. Acta.* 1468:359–366.
10. Huang, C., and J. T. Mason. 1986. Structure and properties of mixed-chain phospholipid assemblies. *Biochim. Biophys. Acta.* 864:423–470.
11. Bultmann, T., H. Lin, Z. Wang, and C. Huang. 1991. Thermotropic and mixing behavior of mixed-chain phosphatidylcholines with molecular weights identical with L-α-dipalmitoylphosphatidylcholine. *Biochemistry.* 30:7194–7202.
12. Durvasula, R. V., and C. Huang. 1999. Thermotropic phase behavior of mixed-chain phosphatidylglycerols: implications for acyl chain packing in fully hydrated bilayers. *Biochim. Biophys. Acta.* 1417: 111–121.
13. Grant, C. W. M., I. E. Mehlhorn, E. Florio, and K. R. Barber. 1987. A long chain spin label for glycosphingolipid studies: transbilayer fatty acid interdigitation of lactosyl ceramide. *Biochim. Biophys. Acta.* 902: 169–177.
14. Mehlhorn, I. E., E. Florio, K. Barber, C. Lordo, and C. W. M. Grant. 1988. Evidence that trans-bilayer interdigitation of glycosphingolipid long chain fatty acids may be a general phenomenon. *Biochim. Biophys. Acta.* 939:151–159.
15. Boggs, J. M., and K. M. Koshy. 1994. Do the long fatty acid chains of sphingolipids interdigitate across the center of a bilayer of shorter chain symmetric phospholipids? *Biochim. Biophys. Acta.* 1189:233–241.
16. Nabet, A., J. M. Boggs, and M. Pézolet. 1996. Study by infrared spectroscopy of the interdigitation of C26:0 cerebroside sulfate into phosphatidylcholine bilayers. *Biochemistry.* 35:6674–6683.
17. Boggs, J. M., K. M. Koshy, and G. Rangaraj. 1993. Thermotropic phase behaviour of mixtures of long chain fatty acid species of cerebroside sulfate with different fatty acid chain length species of phospholipid. *Biochemistry.* 32:8908–8922.
18. Boggs, J. M., K. M. Koshy, and G. Rangaraj. 1988. Interdigitated lipid bilayers of long acyl chain species of cerebroside sulfate. A fatty acid spin label study. *Biochim. Biophys. Acta.* 938:373–385.
19. Levin, I. W., T. E. Thompson, Y. Barenholz, and C. Huang. 1985. Two types of hydrocarbon chain interdigitation in sphingomyelin bilayers. *Biochemistry.* 24:6282–6286.
20. Holopainen, J. M., M. Subramanian, and P. K. J. Kinnunen. 1998. Sphingomyelinase induces lipid microdomain formation in a fluid phosphatidylcholine/sphingomyelin membrane. *Biochemistry.* 37:17562–17570.
21. Bai, J., and R. E. Pagano. 1997. Measurements of spontaneous transfer and transbilayer movement of Bodipy-labeled lipids in lipid vesicles. *Biochemistry.* 36:8840–8848.
22. Contreras, F. X., G. Basañez, A. Alonso, A. Herrmann, and F. M. Goñi. 2005. Asymmetric addition of ceramides but not dihydroceramides promotes transbilayer (flip-flop) lipid motion in membranes. *Biophys. J.* 88:349–359.
23. Lopez-Montero, I., N. Rodriguez, S. Cribier, A. Pohl, M. Velez, and P. F. Devaux. 2005. Rapad transbilayer movement of ceramides in phospholipid vesicles and in human erythrocytes. *J. Biol. Chem.* 280: 25811–25819.
24. Luberto, C., and Y. A. Hannun. 2000. Use of short-chain ceramides. *Methods Enzymol.* 312:407–420.
25. Shabbits, J. A., and L. D. Mayer. 2003. Intracellular delivery of ceramide lipids via liposome enhances apoptosis in vitro. *Biochim. Biophys. Acta.* 1612:98–106.
26. Tokumasu, F., A. J. Jin, and J. A. Dvorak. 2002. Lipid membrane phase behaviour elucidated in real time by controlled environment atomic force microscopy. *J. Electron Microsc.* 51:1–9.
27. Carrer, D. C., S. Härtel, H. L. Monaco, and B. Maggio. 2003. Ceramide modulates the lipid membrane organization at molecular and supramolecular levels. *Chem. Phys. Lipids.* 122:147–152.
28. Fang, Y., and J. Yang. 1997. The growth of bilayer defects and the induction of interdigitated domains in the lipid-loss process of supported phospholipid bilayers. *Biochim. Biophys. Acta.* 1324:309–319.
29. Swamy, M. J., U. Würz, and D. Marsh. 1995. Phase polymorphism, molecular interactions and miscibility of binary mixtures of dimyristoyl-*n*-biotinylphosphatidylethanolamine with dimyristoylphosphatidylcholine. *Biochemistry.* 34:7295–7302.
30. Hubbell, W. L., and H. M. McConnell. 1971. Molecular motion in spin-labeled phospholipids and membranes. *J. Am. Chem. Soc.* 93:314–326.

31. Theodoropoulou, E., and D. Marsh. 2000. Effect of angiotensin II nonpeptide AT1 antagonist losartan on phosphatidylethanolamine membranes. *Biochim. Biophys. Acta.* 1509:346–360.

32. Marsh, D., A. Watts, and I. C. P. Smith. 1983. Dynamic structure and phase behaviour of dimyristoylphosphatidylethanolamine bilayers studied by deuterium nuclear magnetic resonance. *Biochemistry.* 22: 3023–3026.

33. McIntosh, T. J. 1980. Differences in hydrocarbon chain tilt between hydrated phosphatidylethanolamine and phosphatidylcholine bilayers. A molecular packing model. *Biophys. J.* 29:237–245.

34. Seddon, J. M., R. H. Templer, N. A. Warrender, Z. Huang, G. Cevc, and D. Marsh. 1997. Phosphatidylcholine-fatty acid membranes: effects of headgroup hydration on the phase behaviour and structural parameters of the gel and inverse hexagonal (H(II)) phases. *Biochim. Biophys. Acta.* 1327:131–147.

35. Huang, H., E. M. Goldberg, and R. Zidovetzki. 1996. Ceramide induces structural defects into phosphatidylcholine bilayers and activates phospholipase A_2. *Biochem. Biophys. Res. Commun.* 220: 834–838.

36. Holopainen, J. M., J. Y. A. Lehtonen, and P. K. J. Kinnunen. 1997. Lipid microdomains in dimyristoylphosphatidylcholine-ceramide liposomes. *Chem. Phys. Lipids.* 88:1–13.

37. Somerharju, P., J. A. Virtanen, and K. H. Cheng. 1999. Lateral organisation of membrane lipids. The superlattice view. *Biochim. Biophys. Acta.* 1440:32–48.

38. Shah, J., J. M. Atienza, R. I. Duclos, Jr., A. V. Rawlings, Z. Dong, and G. G. Shipley. 1995. Structural and thermotropic properties of synthetic C16:0 (palmitoyl) ceramide: effect of hydration. *J. Lipid Res.* 36:1936–1944.

39. Huang, H., E. M. Goldberg, and R. Zidovetzki. 1998. Ceramides perturb the structure of phosphatidylcholine bilayers and modulate the activity of phospholipase A_2. *Eur. Biophys. J.* 27:361–366.

40. Veiga, M. P., F. M. Goñi, A. Alonso, and D. Marsh. 2000. Mixed membranes of sphingolipids and glycerolipids as studied by spin-label ESR spectroscopy. A search for formation. *Biochemistry.* 39:9876–9883.

41. Sackmann, E. 1995. Physical basis of self-organization and function of membranes: physics of vesicles. *In* Structure and Dynamics of Membranes, Vol 1a. R. Lipowsky and E. Sackmann, editors. Elsevier, Amsterdam. 213–304.